Simple model of the Rayleigh-Taylor instability, collapse, and structural elements

V. P. Goncharov[1] and V. I. Pavlov[2]
[1]*A. M. Obukhov Institute of Atmospheric Physics PAS, 109017 Moscow, Russia*
[2]*UFR des Mathématiques Pures et Appliquées – LML CNRS UMR 8107, Université de Lille 1, 59655 Villeneuve d'Ascq, France*
(Received 28 April 2013; published 6 August 2013)

The mechanisms and structural elements of the Rayleigh-Taylor instability whose evolution results in the occurrence of the collapse have been studied in the scope of the rotating shallow water model with horizontal density gradient. Analysis of the instability mechanism shows that two collapse scenarios are possible. One scenario implies anisotropic collapse during which the contact area of a collapsing fragment with the bottom contracts into a spinning segment. The other implies isotropic contracting of the area into a point. The rigorous integral criteria and power laws of collapses are found.

DOI: 10.1103/PhysRevE.88.023002 PACS number(s): 47.20.Cq, 47.10.Df, 47.20.Ma

I. INTRODUCTION

There exist situations when a fluid dynamic system quickly transitions from its initial stable equilibrium state to an unstable one as a result of change of external governing conditions or of the system control parameters. The most notable example is the Rayleigh-Taylor instability (RTI). The classic (the simplest) RTI occurs when a fluid with lower density accelerates a fluid of higher density, or when a higher density fluid is positioned above a fluid with lower density in a gravitational field or in an accelerating frame of reference. It is a dynamic process where the two fluids seek to reduce their combined potential energy. An initial perturbation (of small magnitude) of the interface between fluids starts in the exponential regime (described by linear differential equations for interface deformation), proceeds to the nonlinear regime, and finally enters a turbulent regime where multiple space scales emerge. Understanding of the dynamics of this process is crucial to the understanding of many phenomena of combustion processes in astrophysical and geophysical environments, the inertial (laser) fusion, accelerating medium of variable density, two-phase flows, and many other phenomena.

One should distinguish between two limit cases based on the ratio of thickness l of the fluid layer ("vertical" size of the container) and the characteristic space scale of initial horizontal deformation of the interface k^{-1} ("horizontal" size of the container): "deep" $kl \gg 1$ and "shallow" $kl \ll 1$ fluids.

In the case of $kl \gg 1$, a small initial sinusoidal deformation of "deep" fluid interface $h(x,0) \sim \sin kx$ with $kh(x,0) \ll 1$ initially grows as $h(x,t) \simeq h(x,0) \exp \Gamma t$ with the growth rate (for a single-mode k) $\Gamma = \sqrt{Agk}$ (when one neglects surface tension). Here, k^{-1} is the horizontal perturbation space scale in the single-mode approximation, g is the gravity or inertial acceleration directed from the h fluid to the l fluid, dimensionless parameter $A = (\varrho_h - \varrho_l)/(\varrho_h + \varrho_l) > 0$ is the Atwood number, ϱ_h and ϱ_l are the densities of the heavier and lighter fluids, respectively, and $h(x,0)$ is the factor that defines the initial single-mode magnitude. When the initial deformation of the interface is not single mode, in the regime with exponential growth each perturbation mode develops independently and is described by linear stability theory [1]. As the deformation of the interface becomes large, $kh(x,t) \simeq 1$, the fluid interface is transformed prior to transitioning to the turbulent regime of the interface motion into "spikes" (where the heavier fluid penetrates the lighter fluid) and "bubbles" (where the lighter fluid rises into the heavier fluid) [2–4].

In this work we focus attention on the other limit case, the so-called "shallow-water"-like approximation (SWL) with $kl \ll 1$. The SWL approximation arises in many physical situations when the characteristic horizontal scale perpendicular to the imposed external (for example, gravity) acceleration **g** is much larger than the vertical dimension of the flow, or when the collinear to **g** component of fluid velocity is strongly suppressed for some reason. In this case the fluid dynamic description can be drastically simplified, permitting the use of simplified models. So, in astro- and geophysical fluid dynamics, many oceanic and atmospheric large-scale currents, flows in rivers, avalanches, and so on, may be investigated using layered models in which the continuous vertical structure is approximated by a small stack of layers with varying thicknesses [5]. In the simplest approximation, the fluid variables within each layer, such as density and horizontal flow velocity, are considered to be vertically uniform, depending only on horizontal coordinates and time. The simplest layer model is the SWL model which describes a single layer of incompressible fluid with a free surface. Finer effects, for example, baroclinic effects due to unaligned density and pressure gradients in a continuously stratified fluid, may be modeled using two or more layers. Inasmuch as layer models with constant layer densities in general have difficulty representing thermodynamic phenomena such as heating or fresh medium forcing that can become important, Ripa [6] proposed to consider a family of layered models that permitted horizontal variations in fluid density within each layer. These density variations may be attributed, for example, to horizontal temperature gradients. In the ocean and atmosphere, gravity currents are driven by temperature and salinity inhomogeneities, or considered as turbidity currents whose density derives from suspended mud or silt [5].

Besides geophysical fluid dynamics, the classical SWL models can be useful for studying certain astrophysical phenomena. For example, a SWL analog was used to describe the shock instability taking place in the collapsing inner core prior to explosion of a protoneutron star [7]. The SWL model can also describe the dynamics of the tachocline of

a star, as was done in [8] and [9] for the tachocline of the Sun. The tachocline is a thin layer of the star's interior, straddling the convection zone and the radiative interior. The tachocline is divided into two sublayers: an inner "radiative" layer and an outer "overshoot" layer. Both sublayers have stable subadiabatic temperature gradients, but the overshoot layer is much closer to being adiabatic. In [8] and [9], the fluid was treated as ideal and the flows as very subsonic, so acoustic compressibility was ignored. The simplest shallow-water system was considered—with one layer of variable thickness, a "free" surface at the top and a rigid boundary at the bottom. It was noted that, in the solar case, the more significant role is played by the boundary between the two layers of the tachocline, rather than the boundary between the tachocline and the convection zone. The convection zone, being adiabatic or superadiabatic, offers no buoyancy resistance to a bulge from below, but the stable subadiabatic stratification within the tachocline provides some *negative stratification* in an amount proportional to the "subadiabaticity" of the layer. Thus, small fluctuations of the temperature regime can shift the system from a state with positive buoyancy to a state with *negative buoyancy*, leading to the hydrodynamical instability of the system.

For SWL flows, as well as for many other nonlinear systems, the problem of stability is central because development of instability determines the possible final regimes realized in the flows. These outcomes depend on the specifics of the model and the initial conditions (integrals of motion). Various scenarios of instability exist, and one of them is the collapse mostly referred to as the "blowup." The extensive literature on this phenomenon is reviewed in [10–15]. This phenomenon implies formation of finite-time singularities and is a rather universal mechanism by which instabilities manifest themselves in nonlinear physical systems [16–23]. In addition, there is good reason to believe that collapses can be key to the understanding of strong turbulence [24–26].

The basic premise of this paper assumes that the development of large-scale instability leads to disintegration of flow and to the occurrence of droplike fluid fragments. In following stages, these quasiregular formations play the role of structural elements from which it is possible to compile an overall picture of the instability up to the final stage when collapse initiating small-scale turbulence is involved in the game. The main goal of this work is to study the scenarios and structural elements of collapses in the well-known shallow-water models. By virtue of the general relativity principle, the results obtained in this paper obviously hold for both a system in a homogeneous gravity field $\mathbf{g}$, and for the one moving with acceleration $\dot{\mathbf{V}}(t)$ [thus replacing $\mathbf{g} \to -\dot{\mathbf{V}}(t)$ in all formulas].

One disadvantage of Ripa's models is that they cannot incorporate the effects of the Rayleigh-Taylor instability due to the fact that, by definition, buoyancy is supposed to be positive in each layer. To overcome these limitations, we have proposed a simple one-layer model [23], whose dynamics is described by a relative buoyancy of alternating sign. As shown therein, an interesting phenomenon, the so-called collapse (blowup), is possible only under certain initial conditions when the integral criterion is fulfilled and the distribution of density (temperature) is such that the potential energy integral is nonpositive. This means that the mechanism responsible for initiating the collapse is the Rayleigh-Taylor instability. Undoubtedly, sooner or later the collapse leads to small-scale processes which the simplified model [23] ignores. However, it is extremely unlikely that in a more complete dissipation-free model the solutions would change so dramatically that collapses would be completely avoided. In particular, as shown in [19,22], accounting for nonlinear dispersion due to nonhydrostatic pressure effects does not suppress the occurrence of collapses in shallow-water models. Even if the collapsing solutions are not explicitly realized (which is most likely due to the loss of self-similarity), the theoretical value of these solutions is that they can be considered as initial or intermediate asymptotics [27].

Work [23] was limited only to the study of integral criteria and power laws of collapses. Finding the space structure for self-similar solutions was outside its scope. In the present work we fill this gap. By analogy with [18–22], it is natural to expect that the development of large-scale instability in the discussed below model also leads to disintegration of the strongly perturbed flow and to the occurrence of droplike fluid fragments. These formations play the role of structural elements that can be used to assess the overall picture of the preturbulence instability. Since the droplike fragments produce space-time singularities responsible for the power-law tails in the short-wave range of the spectrum, the study of the structural elements provides a key to the understanding of strong turbulence [24,25].

The importance of the issue becomes clear in the following historical episode. The well-known Manhattan Project required implementation of a simultaneous and uniform explosive compression of a spherical target of density $\varrho_h \simeq 19.3$ by a spherical layer of less density, $\varrho_l \simeq 19.0$ (Atwood number $A \simeq 0.008 \ll 1$)—this is how the implosion was created. Physically, the behavior of the ϱ_h/ϱ_l interface, which during target compression moves locally with acceleration, is equivalent to the behavior of a fluid in a drinking glass turned upside down (subject to the gravity of Earth). In such a situation, the interface is obviously unstable (Rayleigh-Taylor instability) and quickly deforms producing "fingers" and "spikes." In the sense of "rigorous" mathematics, such a problem is "ill posed." However, the success of the entire Project was critically dependent on the ability to determine the conditions under which the development of this hydrodynamical instability was slower than the rapidity of the implosion; otherwise, instead of a powerful explosion one would get a trivial "whiff." Enrico Fermi and John von Neumann were instrumental in analyzing this problem. Fermi obtained (notably, with the use of a beautifully simple and elegant model) for the magnitude of the surface deformation in the nonlinear regime of evolution one of the most important results for the Project realization: the fact that the time dependence of the instability evolution growth is proportional to the square of time, not exponential and, as we all know, in the end successfully implemented the Project [28]. In modern terms, they were interested exactly in the "collapses" (which is what our paper is about) that appear as jets and bubbles resulting due to Rayleigh-Taylor instability when a heavy fluid sinks into a lighter one.

This article is organized as follows. In Sec. II we construct the minimal model and formulate the governing equations

in the shallow-water approximation with horizontal density gradients. In Sec. III we discuss the rigorous integral criterion for isotropic collapse. We assume that this phenomenon arises at the final stage when the development of instability has led to disintegration of strongly perturbed flows. After the formation of localized fluid fragments, there comes a time when finite-time singularities form. The self-similar scenarios of collapses and their corresponding structural elements are considered in Secs. IV–VI. In Sec. VII we summarize our results.

II. MINIMAL MODEL

To illustrate the concept we consider the simplest model which can be proved within the framework of the two-layer model (see the Appendix for more details). This model supposes that two incompressible fluids with densities $\varrho =$ const and $\varrho + \varrho'(x_1,x_2,t)$ are separated by the interface $z = h(x_1,x_2,t)$ and contained between two rigid parallel planes $z = 0$ and $z = l$ under action of gravity g. When the space-temporally depending density jump ϱ' between the fluids is small and the lower layer is sufficiently thin, so inequalities $\varrho'/\varrho \ll 1$ and $h/l \ll 1$ hold, then we can obtain evolution generalized SWL equations

$$\partial_t u_i + u_k \partial_k u_i - 2\Omega e_{ik} u_k = -\partial_i (h\tau) + \tfrac{1}{2} h \partial_i \tau, \tag{1}$$

$$\partial_t h + \partial_k (h u_k) = 0, \tag{2}$$

$$\partial_t \tau + u_k \partial_k \tau = 0. \tag{3}$$

These equations describe depth-averaged flow in the lower layer. The used notations are as follows: $x_i = (x_1,x_2)$ are the Cartesian coordinates; $\partial_t = \partial/\partial t$, $\partial_i = \partial/\partial x_i$; e_{ik} is the unit antisymmetric tensor, $e_{11} = e_{22} = 0$, $e_{12} = -e_{21} = 1$; $u_i = (u_1,u_2)$ are horizontal components of depth-averaged velocity in layer; and h is its thickness depending on coordinates and time. Hereinafter, summation over repeated indices is implied. Since Ω is constant angular velocity with which the layer is rotating about the vertical axis, the term $2\Omega e_{ik} u_k$ implies components of Coriolis acceleration. The field variable $\tau = g\varrho'/\varrho$ has the meaning of relative buoyancy and therefore may take any sign.

In those cases when density variations are produced only by temperature ones ΔT and are linearly connected, the relative buoyancy can be computed as $\tau = -g\beta\Delta T$, where β is the thermal expansion coefficient. This parametrization allows one to study heating and cooling effects in SWL models [29,30].

Note that in the case $\tau = 1$ Eqs. (1)–(3) reduce to the usual SWL equations. The other limiting case $\tau = -1$ leads to the so-called "inverted" SWL model describing the layer of a heavy fluid bounded above by a solid slab. The equilibrium in the unperturbed state is provided by the pressure of a light fluid or a gas lying below. Examples of using the inverted shallow-water model in various applications are presented in [31]. Understandably, such equilibrium is unstable (the Rayleigh-Taylor instability) and short lived. Eventually the heavier fluid falls down to the bottom. But initial and intermediate stages of the instability, when the system is far from the final state, are of the utmost importance. Their study provides a way for an understanding of the different important processes such as, for example, the processes of vertical mixing in many physical applications, including nuclear physics and atmospheric and ocean science.

There is one more useful interpretation of Eqs. (1)–(3) as equations of hydrodynamic type driven from first principles (conservation laws). As can be verified directly, if variables h and τ are considered as "mass density" and "entropy" (not to be confused with the classical entropy), Eqs. (1)–(3) follow from the Hamiltonian formulation [17,32] of two-dimensional motion of a nonbarotropic rotating gas with the Hamiltonian

$$H = \int d\mathbf{x} \left(h \frac{\mathbf{u}^2}{2} + \epsilon(h,\tau) \right).$$

Here, $\epsilon(h,\tau)$ is an internal energy density which in our case is given by the expression $\epsilon = h^2\tau/2$, and $d\mathbf{x} = dx_1 dx_2$.

In terms of variables h, τ, and

$$\mathbf{m} = \frac{\delta H}{\delta \mathbf{u}} = h\mathbf{u}$$

(referred to as the hydrodynamic momentum density), nontrivial Poisson brackets defining the dynamics for the given family of models take the form

$$\{m_i, m'_k\} = \partial'_i (m'_k \delta) - \partial_k (m_i \delta) + 2h\Omega e_{ik} \delta, \tag{4}$$

$$\{h, m'_k\} = -\partial_k (h\delta), \quad \{\tau, m'_k\} = -\delta \partial_k \tau. \tag{5}$$

Here primed field variables mean the dependence on the primed spatial coordinates, and $\delta = \delta(\mathbf{x} - \mathbf{x}')$ is the Dirac delta function.

Evolution equations (1)–(3) conserve integrals of total mass Q and total energy H,

$$Q = \int d\mathbf{x}\, h, \quad H = \frac{1}{2} \int d\mathbf{x} (h\mathbf{u}^2 + h^2\tau). \tag{6}$$

In addition, any system with the Poisson brackets (4),(5) automatically conserves the integrals (Casimirs)

$$C = \int d\mathbf{x} \left(\partial_1 u_2 - \partial_2 u_1 + 2\Omega \right) F(\tau),$$

for any function $F(\tau)$. Among them we note the conservation law

$$n = \int d\mathbf{x}\, \tau \left(\partial_1 u_2 - \partial_2 u_1 + 2\Omega \right). \tag{7}$$

As we will see, this quantity together with other constants of motion play an important role in determining self-similar solutions considered in Secs. IV-VI.

III. COLLAPSE CRITERION

If the fluid moves as a whole, then it is convenient to go from old coordinates $\mathbf{x}$ to new ones $\mathbf{x}'$ connected with the center of mass reference frame. In this case the primed and unprimed coordinates and velocities are related by the transformation

$$\mathbf{x} = \mathbf{X} + \mathbf{x}', \quad \mathbf{u} = Q^{-1}\mathbf{P} + \mathbf{u}'. \tag{8}$$

Here coordinates of the center of mass $\mathbf{X}$ and components of the total momentum $\mathbf{P}$ are defined as

$$\mathbf{X} = Q^{-1} \int d\mathbf{x}\, h\mathbf{x}, \quad \mathbf{P} = \int d\mathbf{x}\, h\mathbf{u},$$

and on the grounds of Eqs. (1)–(3) are governed by the equations

$$\partial_t X_i = Q^{-1} P_i, \quad \partial_t P_i = 2\Omega e_{ik} P_k.$$

Since the transformation (8) leaves invariant Eqs. (1)–(3), we will not change the notations by merely setting $\mathbf{P} = 0$ and $\mathbf{X} = 0$ from the very beginning.

As shown in [23], the model (1)–(3) admits a simple mechanical reduction in terms of variables

$$V = \int d\mathbf{x}\, h x_i u_i, \quad M = \int d\mathbf{x}\, h\,(x_1 u_2 - x_2 u_1),$$
$$I = \int d\mathbf{x}\, h\mathbf{x}^2. \tag{9}$$

Integrals I, M, and V denote the moment of inertia, the kinetic moment, and the virial, respectively, and obey a closed system of equations

$$\partial_t I = 2V, \quad \partial_t V = 2H + 2\Omega M, \quad \partial_t M = -2\Omega V. \tag{10}$$

Equations (10) give two more motion integrals

$$m = M + \Omega I, \quad V_0^2 = (M + \Omega^{-1} H)^2 + V^2, \tag{11}$$

and can be easily integrated to obtain

$$I = \Omega^{-2}(H + \Omega m) - \frac{V_0}{\Omega}\cos 2\Omega (t - t_0), \tag{12}$$

$$M = -\Omega^{-1} H + V_0 \cos 2\Omega (t - t_0), \tag{13}$$

$$V = V_0 \sin 2\Omega (t - t_0). \tag{14}$$

Here t_0 is a constant of integration.

The integral I serves as an indicator of the isotropic collapse, in the course of which this positive-defined quantity undergoes specific temporal changes: I decreases with increasing t and reaches the value $I = 0$ at a finite point $t = t_0 > 0$. The condition for such behavior is the inequality

$$(H + \Omega m)^2 \leqslant \Omega^2 V_0^2. \tag{15}$$

This inequality is the criterion for collapse in the rotating shallow-water model with horizontally nonuniform density. Only under this condition, the development of instability leads to the formation of a singularity in the point $\mathbf{x} = 0$.

According to (15), the stability of the system is determined by four constants of the motion: H, m, V_0, and Ω. In place of them it is a more suitable to use two nondimensional parameters

$$\nu = \frac{H}{m\Omega}, \quad \upsilon = \left(\frac{V_0}{m}\right)^2,$$

in terms of which the possible scenarios of stability and instability can be analyzed with the diagram shown in Fig. 1.

From the diagram of stability, we see that increasing the angular velocity $|\Omega|$, so $\nu \to 0$ as $|\Omega| \to \infty$, allows the system to leave the collapse region only if $\upsilon \leqslant 1$, i.e., $|V_0| \leqslant |m|$. However in the opposite case $\upsilon > 1$ (and hence $|V_0| > |m|$) under otherwise fixed parameters, an analogous behavior of $|\Omega|$ does not lead to the same result.

Since in the case of isotropic collapsing the h behaves as a self-similar function so that $h = \beta^{-2} f(\mathbf{x}/\beta)$, one can write

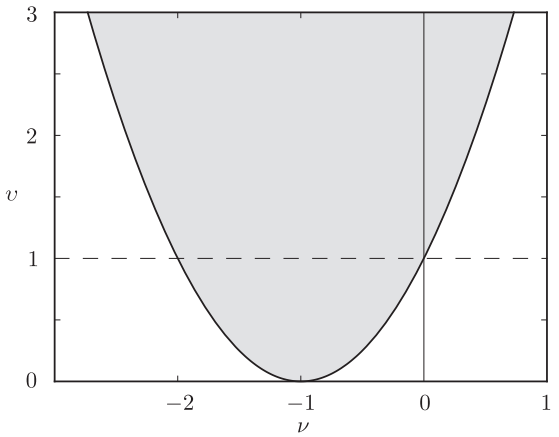

FIG. 1. Stability diagram. The collapse region is indicated by the gray color.

the relation

$$I = \beta^2 C, \tag{16}$$

where $\beta(t)$ is a function of time, and C is a positive constant depending on the shape factor f only.

On the other hand, expanding the function I in powers of $(t_0 - t)$ in the vicinity of the collapse time t_0, we approximately obtain

$$I \approx a_1 (t_0 - t) + a_2 (t_0 - t)^2 + \cdots, \tag{17}$$

where t_0, coefficients a_1,a_2, and integrals of motion are connected by relations

$$a_1 = 2\sqrt{V_0^2 - \Omega^{-2}(H + \Omega m)^2},$$
$$a_2 = 2(H + \Omega m),$$
$$H + \Omega m = V_0 \Omega \cos(2\Omega t_0).$$

Thus, the comparison of (16) with (17) allows us to make the following conclusions.

(1) If $a_1 \neq 0$, i.e., the inequality (15) is strict, then the isotropic collapse obeys laws

$$\beta \sim (t_0 - t)^{1/2}, \quad h \sim \beta^{-2} \sim (t_0 - t)^{-1}. \tag{18}$$

(2) But if $a_1 = 0$, i.e., the inequality (15) turns into equality, then, instead of (18), we obtain the laws

$$\beta \sim (t_0 - t), \quad h \sim \beta^{-2} \sim (t_0 - t)^{-2}.$$

It should be noted that system (10) may be viewed as one of the generalizations of the virial theorem which allows one to get the Vlasov-Petrishchev-Talanov-type criterion for collapse in the nonlinear Schrödinger (NLS) equation. This criterion was first formulated for the two-dimensional NLS equation [33] and later was generalized to many other models. Among them is the NLS model in quasiclassical limit [34] when the Zakharov equations transform into the hydrodynamic type system. In particular, in the absence of rotation, system (10) reduces to the equation

$$\partial_{tt} I = 4H, \tag{19}$$

which coincides with that for the two-dimensional NLS equation, and after integration gives

$$I = 2Ht^2 + I_0' t + I_0. \tag{20}$$

Here, the initial data $I_0 = I|_{t=0}$ and $I_0' = (\partial_t I)|_{t=0} = 2V|_{t=0}$ are used as constants of integration. In this case the criterion (17) reads as

$$2HI \leqslant V^2 = \tfrac{1}{4}\left[(\partial_t I)\right]^2 \tag{21}$$

and enables us to make the following conclusions.

(1) If $H < 0$, the isotropic collapse occurs always. Since H can be represented as

$$H = K + \Pi, \quad K = \frac{1}{2}\int d\mathbf{x}\, h\mathbf{u}^2, \quad \Pi = \frac{1}{2}\int d\mathbf{x}\, h^2\tau, \tag{22}$$

the inequality $H < 0$ implies that $\Pi|_{t=0} < K|_{t=0}$. The only way to provide this condition is by appropriately choosing the initial distribution for field τ which, unlike h, can be sign alternating.

(2) If $H \geqslant 0$, the fulfillment of criterion (22) depends on I_0 and I_0', so at initial time we have the condition

$$8HI_0 \leqslant (I_0')^2, \tag{23}$$

where I_0' must be negative because I decreases with time.

On the other hand, on the base of the Cauchy inequality we can write

$$(\partial_t I)^2 = 4V^2 \leqslant 8IK. \tag{24}$$

It is clear that inequalities (23) and (24) are consistent only if

$$H \leqslant \frac{(I_0')^2}{8I_0} \leqslant K|_{t=0}. \tag{25}$$

As a consequence, we come to the condition $K|_{t=0} \leqslant \Pi|_{t=0} \leqslant 0$. Therefore, irrespective of the sign of H, the collapse becomes possible, if only $\Pi|_{t=0} \leqslant 0$. The negative quantity $-K|_{t=0}$ plays the role of a critical level. For values $\Pi|_{t=0}$ below the critical level no conditions are required, but above or at this level the additional conditions must be met.

IV. STRUCTURAL ELEMENTS OF COLLAPSES

As known [27], self-similar solutions are intermediate asymptotics of nondegenerate problems and are very useful in studying the final stages of strongly nonlinear processes, when the system forgets about details related to the initial data and its behavior depends on the motion integrals. For any dynamical system, the existence of self-similar solutions reflects the existence of fundamental internal symmetries and allows us to judge the tendencies in the development of the instability at the final stage. This type of solution is of particular importance for studying the phenomenon of collapse—the formation of a singularity in a finite time [10–15,34].

As a self-similar substitution for h and τ we consider expressions

$$h = \frac{Q|G|}{\pi}(1+\gamma)f^{\gamma}, \quad \tau = \tau_0 f^{1-\gamma}, \tag{26}$$

$$f = 1 - (GU\mathbf{x})^2. \tag{27}$$

Here, exponent γ satisfies $0 \leqslant \gamma \leqslant 1$, τ_0 is a magnitude-specified parameter, G and U are dilatation and rotation matrices

$$G = \begin{pmatrix} \beta_1^{-1} & 0 \\ 0 & \beta_2^{-1} \end{pmatrix}, \quad U = \begin{pmatrix} \cos\varphi & -\sin\varphi \\ \sin\varphi & \cos\varphi \end{pmatrix},$$

$\beta_1(t)$ and $\beta_2(t)$ are positive deformation parameters, and variable $\varphi(t)$ is the angle of rotation in transformation $\mathbf{x}' = U\mathbf{x}$.

The ansatz (26), (27) describes a liquid drop concentrated on a compact carrier of elliptic shape

$$x_1'^2\beta_1^{-2} + x_2'^2\beta_2^{-2} = 1,$$

and rotated with the angular speed $\partial_t\varphi$.

Direct substitution into Eqs. (1)–(3) shows that expressions (26) and (27) are exact solutions if in the rotating coordinate system $\mathbf{x}' = U\mathbf{x}$ velocity components $\mathbf{u}' = d\mathbf{x}'/dt$ obey the relations

$$u_1' = \frac{\alpha_1}{\beta_1}x_1' - \lambda\frac{\beta_1}{\beta_2}x_2', \quad u_2' = \frac{\alpha_2}{\beta_2}x_2' + \lambda\frac{\beta_2}{\beta_1}x_1'. \tag{28}$$

Equations (28) correspond to the uniform vorticity distribution inside the domain with elliptical liquid contour boundary. Variables α_i, β_i, λ, and $\varphi' = \varphi - \Omega t$ as functions of time satisfy equations

$$\partial_t\alpha_i = -\beta_i\Omega^2 + (-1)^i 2(\beta_2 - \beta_1)\lambda\partial_t\varphi' + \beta_i(\lambda - \partial_t\varphi')^2 + \frac{Q\tau_0(1+\gamma)^2}{\pi\beta_i\beta_1\beta_2}, \tag{29}$$

$$\partial_t\beta_i = \alpha_i, \tag{30}$$

$$m' = \lambda\beta_1\beta_2 - \tfrac{1}{2}\left(\beta_1^2 + \beta_2^2\right)\partial_t\varphi', \tag{31}$$

$$n' = \tfrac{1}{2}\lambda\left(\beta_1^2 + \beta_2^2\right) - \beta_1\beta_2\partial_t\varphi'. \tag{32}$$

Here m' and n' are parameters connected with motion invariants m and n by relations

$$m' = (2+\gamma)\frac{m}{Q}, \quad n' = (2-\gamma)\frac{n}{2\pi\tau_0}.$$

Note that Eqs. (31) and (32) can be alternatively derived by substituting (26), (27), and (28) into the right-hand sides of (7) and (11).

After eliminating variables λ,φ' from Eqs. (29)–(32), we find that variables α_i and β_i obey the canonical equations of motion

$$\partial_t\alpha_i = -\frac{\partial\mathscr{H}}{\partial\beta_i} = -\beta_i\Omega^2 + 2\frac{(n'+m')^2}{(\beta_1+\beta_2)^3} - (-1)^i 2\frac{(n'-m')^2}{(\beta_1-\beta_2)^3} + \frac{Q\tau_0(\gamma+1)^2}{\pi\beta_i\beta_1\beta_2}, \tag{33}$$

$$\partial_t\beta_i = \frac{\partial\mathscr{H}}{\partial\alpha_i} = \alpha_i, \tag{34}$$

which describe a system with two degrees of freedom and Hamiltonian

$$\mathscr{H} = 2\frac{(\gamma+2)}{Q}(H + \Omega m) = \frac{1}{2}\left(\alpha_1^2 + \alpha_2^2\right) + \left(\frac{n'+m'}{\beta_1+\beta_2}\right)^2 + \left(\frac{n'-m'}{\beta_1-\beta_2}\right)^2 + \frac{\Omega^2}{2}\left(\beta_1^2 + \beta_2^2\right) + \frac{Q\tau_0(1+\gamma)^2}{\pi\beta_1\beta_2}. \tag{35}$$

Once we know variables β_1 and β_2, we can find variables λ and $\partial_t\varphi$:

$$\lambda = 2\frac{n'\left(\beta_1^2+\beta_2^2\right)-2m'\beta_1\beta_2}{\left(\beta_1^2-\beta_2^2\right)^2},$$
$$\partial_t\varphi = \Omega + 2\frac{2n'\beta_1\beta_2 - m'\left(\beta_1^2+\beta_2^2\right)}{\left(\beta_1^2-\beta_2^2\right)^2}.$$

Thus, ansatz (26),(27),(28) reduces the initial infinite-dimensional Hamiltonian system given by Eqs. (1)–(3) to a two-dimensional canonical system.

If motion invariants n and Ω are finite, it is convenient to convert the problem to dimensionless form by choosing spatial scale L and characteristic time T so that

$$T = |\Omega|^{-1}, \quad L = |n'/\Omega|^{1/2}.$$

After nondimensionalizing, Hamiltonian (35) is rewritten as

$$\mathscr{H} = \frac{1}{2}\left(\alpha_1^2+\alpha_2^2+\beta_1^2+\beta_2^2\right) + \frac{\sigma-1}{\beta_1\beta_2} + \left(\frac{1+\mu}{\beta_1+\beta_2}\right)^2 + \left(\frac{1-\mu}{\beta_1-\beta_2}\right)^2,$$

where μ and σ are the nondimensional parameters

$$\mu = \frac{m'}{n'} = 2\pi\frac{(2+\gamma)}{(2-\gamma)}\frac{\tau_0 m}{Qn},$$
$$\sigma = 1 + 4\pi\left(\frac{1+\gamma}{2-\gamma}\right)^2\frac{Q\tau_0^3}{n^2}. \tag{36}$$

The corresponding equations of motion for α_i, β_i, and φ are given by

$$\partial_t\alpha_i = -\frac{\partial\mathscr{H}}{\partial\beta_i} = -\beta_i + \frac{\sigma-1}{\beta_i\beta_1\beta_2} + 2\frac{(1+\mu)^2}{(\beta_1+\beta_2)^3} - (-1)^i 2\frac{(1-\mu)^2}{(\beta_1-\beta_2)^3}, \tag{37}$$

$$\partial_t\beta_i = \frac{\partial\mathscr{H}}{\partial\alpha_i} = \alpha_i, \tag{38}$$

$$\partial_t\varphi = 1 + 2\,\mathrm{sign}\,(n')\frac{2\beta_1\beta_2 - \mu\left(\beta_1^2+\beta_2^2\right)}{\left(\beta_1^2-\beta_2^2\right)^2}. \tag{39}$$

V. ISOTROPIC SOLUTIONS

Below we will discriminate isotropic solutions of two types: rotating ($\Omega = 1$) and nonrotating ($\Omega = 0$).

Let $\Omega = 1$, and assume that solutions are radially symmetric. Hence

$$\beta_1 = \beta_2 = \beta, \quad \alpha_1 = \alpha_2 = \alpha.$$

As analysis shows such solutions are degenerate and are possible only if $\mu = 1$ or $m' = n'$. This is the reason why the rotational effect due to $\partial_t\varphi$ loses theoretical legitimacy and Eq. (39) is no longer valid. Instead, one can see directly from (31) and (32) that functions φ and λ become linearly dependent:

$$\mu = 1 = \beta^2\left(1+\lambda-\partial_t\varphi\right).$$

Thus isotropic solutions are rotationally invariant.

In this case Eqs. (37) and (38) reduce to the following form:

$$\partial_t\alpha = -\frac{\partial H_1}{\partial\beta} = \frac{\sigma}{\beta^3} - \beta, \quad \partial_t\beta = \frac{\partial H_1}{\partial\alpha} = \alpha, \tag{40}$$

where

$$H_1 = \frac{1}{2}\left(\alpha^2+\beta^2+\frac{\sigma}{\beta^2}\right). \tag{41}$$

The analytical solutions of Eq. (40) can be written as

$$\beta = \sqrt{H_1 - \left(H_1^2-\sigma\right)^{1/2}\cos 2(t_0-t)},$$
$$\alpha = \frac{\left(H_1^2-\sigma\right)^{1/2}\sin 2t(t_0-t)}{\sqrt{H_1 - \left(H_1^2-\sigma\right)^{1/2}\cos 2(t_0-t)}}. \tag{42}$$

Relevant structures look like radially symmetric drops.

Without loss of generality we can assume that σ equals either 0, 1, or -1. On condition that $\Omega = 1$, depending on the parameter σ, there are three different branches of solutions, hereafter referred to as neutral ($\sigma = 0$), cold ($\sigma = 1$), and warm ($\sigma = -1$) rotating regimes. The parameter σ is chosen according to the rule

$$\sigma = \begin{cases} 0, & \text{if} \quad \tau_0 = \tau^* \\ 1, & \text{if} \quad \tau_0 > \tau^* \\ -1, & \text{if} \quad \tau_0 < \tau^*; \end{cases}$$

where the threshold value τ^* is determined from (36) subjected to condition $\sigma = 0$, which yields

$$\tau^* = -\left(\frac{n^2}{4\pi Q}\right)^{1/3}\left(\frac{2-\gamma}{1+\gamma}\right)^{2/3}.$$

(1) In the neutral regime, when $\sigma = 0$, the motion can occur only if $H_1 > 0$. As shown in Fig. 2, the system moves along open trajectories in the form of semicircles. The arrows placed along the phase trajectories represent the direction of motion in time. Relevant solutions for h look like drops collapsing

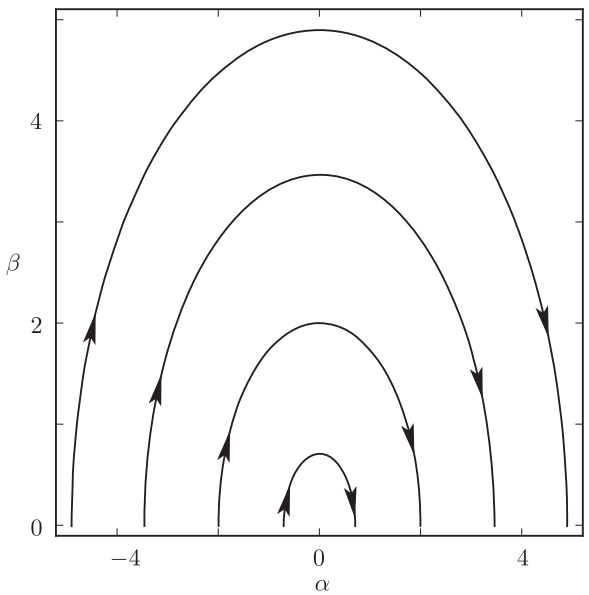

FIG. 2. Phase portrait of the rotating isotropic model in the neutral regime ($\sigma = 0$).

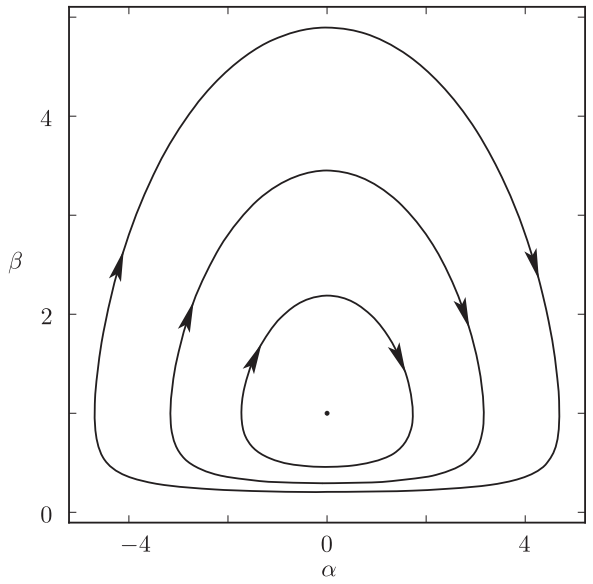

FIG. 3. Phase portrait of the rotating isotropic model in the cold regime ($\sigma = 1$).

according to laws

$$\beta \sim t_0 - t, \quad \alpha \sim -\sqrt{2H_1}, \quad h \sim (t_0 - t)^{-2}.$$

(2) In the cold regime, the motion can occur only if $H_1 \geqslant 1$. According to Fig. 3, the typical trajectories of the dynamical system are depicted by closed curves which correspond to periodic solutions. Relevant solutions for h look like pulsating drops. The minimum $H_1 = 1$ is attained at the point $\alpha = 0$, $\beta = 1$ and corresponds to a stationary (nonpulsating) solution.

(3) In the warm regime, the system moves along open trajectories shown in Fig. 4. The collapse point is reached for both positive and negative values of H_1 when $\alpha \to \infty$ and $\beta \to 0$. In this regime variable β and α asymptotically (as $t \to t_0$) tend to zero and infinity, respectively, according to the

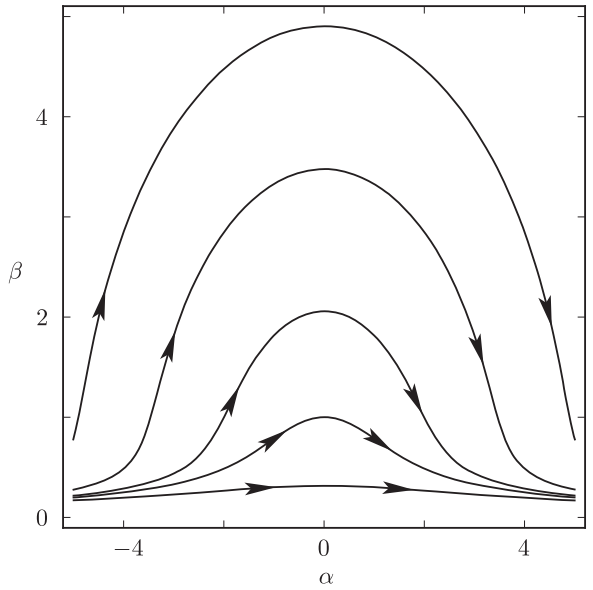

FIG. 4. Phase portrait of the rotating isotropic model in the warm regime ($\sigma = -1$).

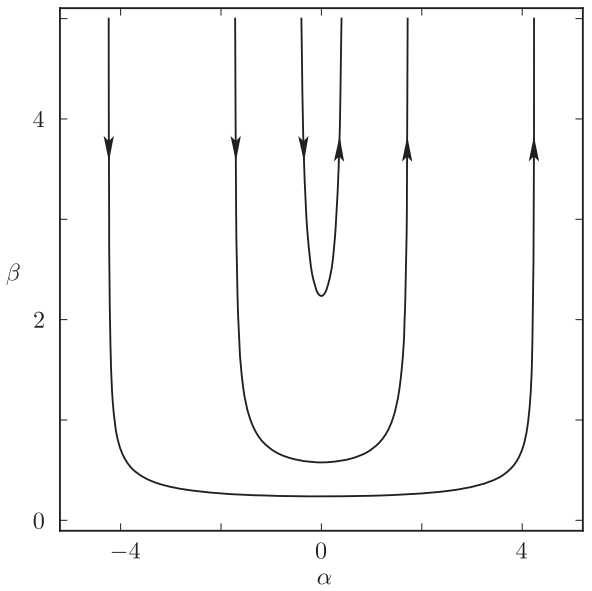

FIG. 5. Phase portrait of the nonrotating isotropic model in the cold regime ($\sigma = 1$).

following laws:

$$\beta \sim (t_0 - t)^{1/2}, \quad \alpha \sim (t_0 - t)^{-1/2}, \quad h \sim (t_0 - t)^{-1},$$

where collapse time

$$t_0 = \frac{1}{2} \arccos \frac{H_1}{\sqrt{1 + H_1^2}}$$

is determined from (42) on the condition that $\beta(t_0) = 0$.

It is worth emphasizing that in the case $\Omega = 1$ among solutions of Eqs. (40) there are no spreading regimes for which $\beta \to \infty$ at $t \to \infty$. These regimes occur only in nonrotating shallow-water models when $\Omega = 0$. Since the proper analytical treatment implies dropping from Hamiltonian (41) the term with β^2, Eqs. (40) are reduced to form

$$\partial_t \alpha = -\frac{\partial H_0}{\partial \beta} = \frac{\sigma}{\beta^3}, \quad \partial_t \beta = \frac{\partial H_0}{\partial \alpha} = \alpha, \tag{43}$$

where

$$H_0 = \frac{1}{2}\left(\alpha^2 + \frac{\sigma}{\beta^2}\right).$$

Phase trajectories of Eqs. (43) are presented in Figs. 5 and 6 for both cold and warm nonrotating regimes. The steady-state case $\sigma = 0$ is of no interest because of its triviality. Regardless of the sign of the parameter σ, spreading regimes are realized only on trajectories with $H_0 > 0$. In Fig. 6 the spreading ($H_0 > 0$) and collapsing ($H_0 < 0$) regimes are separated by the dashed line. Thus, if $\sigma = -1$ (i.e., a regime is warm) and $H_0 < 0$, the topology of phase trajectories does not depend on whether the shallow-water model is rotating or not.

VI. ANISOTROPIC SOLUTIONS

Eqs. (37) and (38) can have solutions that violate the radial symmetry. In such situations, using positive definite integral (9) to test the anisotropic collapse is not a good

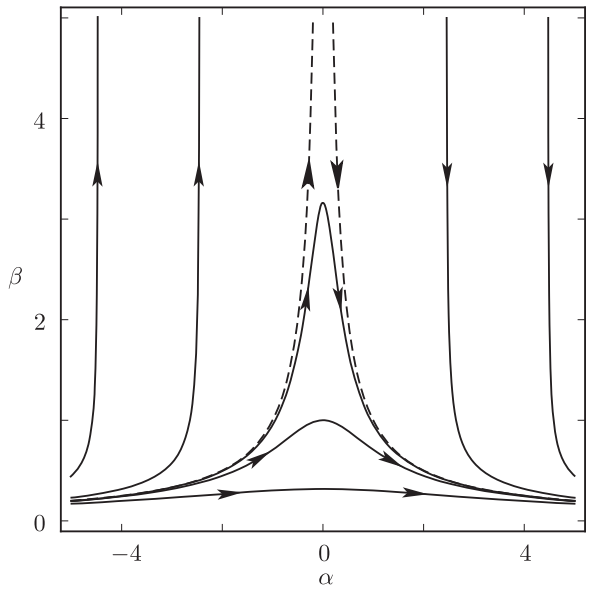

FIG. 6. Phase portrait of the nonrotating isotropic model in the warm regime ($\sigma = -1$).

idea, since this quantity reaches zero only if β_1 and β_2 vanish simultaneously.

First of all, we consider the anisotropic collapse scenario, according to which the cross sectional area ($s = \pi\beta_1\beta_2$) tends to zero due to the unilateral compression along one of the semiaxes (e.g., β_1), whereas the other semiaxis β_2 remains finite (Fig. 7). As a result, the elliptic contact area of a collapsing liquid fragment contracts into a line segment rather than into a point.

Analysis of the anisotropic collapse solutions in the vicinity of point $t = t_0$ results in the following asymptotics for

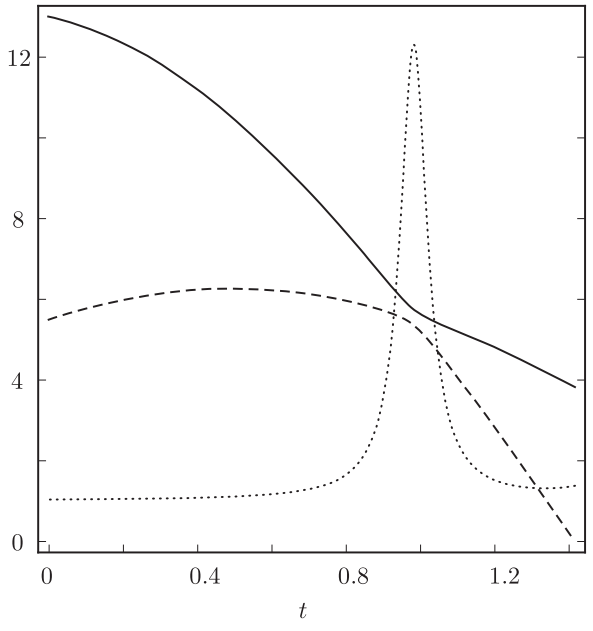

FIG. 7. Anisotropic collapse. The solid, dashed, and dotted lines are β_2, β_1, and $\partial_t\varphi$, respectively. The calculation was performed for the parameters $\sigma = -4$, $\mu = 2.8$, and the following initial values: $\beta_1(0) = 5.5$, $\beta_2(0) = 13$, $\alpha_1(0) = 3$, $\alpha_2(0) = -2$.

β_1 and β_2:

$$\beta_1 \approx b\,(t_0 - t)^{2/3} + a\,(t_0 - t)^{4/3}\,, \tag{44}$$

$$\beta_2 \approx -\frac{9}{2}b^{-3}(\sigma - 1) + \frac{b^5}{9(\sigma - 1)}\,(t_0 - t)^{4/3}\,. \tag{45}$$

Here b and a are constants dependent on the initial conditions and closely connected with other constants of motion by the relationship

$$H = \frac{3^4\,(\sigma - 1)^2}{2^3\,b^6} + b^6\frac{2^3}{3^4}\frac{1 + \mu^2}{(\sigma - 1)^2} + \frac{10}{9}ba.$$

Asymptotics (44) and (45) denote two things. First, the anisotropic collapse is possible only if $\sigma < 1$ and, correspondingly, requires a negative value of τ_0. Second, since $h \sim (\beta_1\beta_2)^{-1}$, such collapse obeys the law

$$h \sim (t_0 - t)^{-2/3}\,.$$

In contrast, the isotropic collapses follow the comparatively quicker laws $h \sim (t_0 - t)^{-1}$ or $h \sim (t_0 - t)^{-2}$.

Note that when $t \to t_0$ the contact area s between liquid and bottom shrinks into the line segment which rotates with the constant angular velocity

$$\partial_t\varphi = 1 - 2\mu\beta_2^{-2} = 1 - \frac{2^3}{3^4}\frac{\mu b^6}{(\sigma - 1)^2}.$$

Collapsing solutions in the flat model have the same character as in the 2D model, with the only difference being that the contact area s shrinks not into a line segment but into an infinite axis perpendicular to the flow plane.

The flat model for shallow water follows from Eqs. (33) and (34) if one of the semiaxes (e.g., β_2) and, correspondingly, the total mass Q tend to infinity on the condition that $Q/\beta_2 \to$ const, $\alpha_2 \to 0$, $\Omega = n = m = 0$. Thus collapses in the flat model represent an idealization that ignores the effects of rotation.

In this case the nondimensional equations of motion are written as

$$\begin{gathered}\partial_t\alpha_1 = -\frac{\partial H'}{\partial\beta_1} = \frac{\sigma}{\beta_1^2}, \quad \partial_t\beta_1 = \frac{\partial H'}{\partial\alpha_1} = \alpha_1, \\ H' = \frac{1}{2}\alpha_1^2 + \frac{\sigma}{\beta_1},\end{gathered} \tag{46}$$

where $\sigma = \operatorname{sign}\tau_0$ is the only nondimensional parameter.

Phase portraits of nonlinear system (46) have no qualitative distinctions from the ones presented in Figs. 5 and 6. As analysis shows, depending on the parameter σ, there exist two kinds of collapsing regimes. If $\sigma < 0$, variables β and h asymptotically (as $t \to t_0$) tend to zero and infinity, respectively, according to the law

$$\beta_1 \sim (t_0 - t)^{2/3}, \quad h \sim (t_0 - t)^{-2/3}.$$

But, if $\sigma = 0$, these variables obey the law

$$\beta_1 \sim (t_0 - t), \quad h \sim (t_0 - t)^{-1}.$$

In the absence of collapses, the system (37)–(39) describes nonlinear oscillation. Such behavior of the system agrees completely with laws (12)–(14), according to which the oscillatory period π/Ω is indispensable for the rotating shallow water

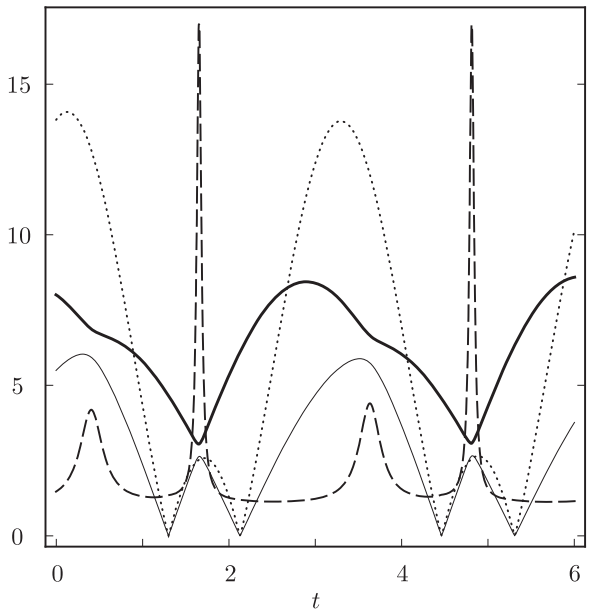

FIG. 8. Oscillation regime. The thick and thin solid lines are β_2 and β_1, the dashed and dotted lines are $\partial_t\varphi$ and $s/10$. The calculation was performed for the parameters $\sigma = 2$, $\mu = 3.8$, and the following initial values: $\beta_1(0) = 5.5$, $\beta_2(0) = 8$, $\alpha_1(0) = 3$, $\alpha_2(0) = -2$.

model. Because this period defines the maximum time scale in the system, characteristic times of all other feasible effects, including collapse, should be smaller.

A typical example of time behavior for basic functions is shown in Fig. 8. In spite of the fact that collapse is physically impossible ($\sigma > 1$), the minimal and maximal values of area s (height h) can be very small and very large. Specifically, the numerical experiment in Fig. 8 gives $s_{\max} = 137.76$ and $s_{\min} = 0.095$. Another fact drawing attention is the periodic bursts of the angular velocity $\partial_t\varphi$ (marked by a dashed line) at the instant when the semiaxes β_1 and β_2 come close to each other.

VII. CONCLUSIONS

In summary, this paper deals with investigations of collapse in the system of two fluid layers when the flow of the lower layer (its density is assumed constant) is described in the shallow-water approximation, and the upper layer has the density fluctuation ϱ' depending on the horizontal coordinates. In such a case the system can undergo Rayleigh-Taylor instability which is the main reason for collapse in this system. Furthermore, the authors assume the existence of constant rotation in the horizontal plane with the frequency Ω. As shown in this paper, the system motion is described by three two-dimensional equations: the continuity equation for the lower layer height h, analogous to that for the shallow-water limit for one layer, the equation for the density fluctuation of the upper layer showing that the density fluctuation is the Lagrangian invariant, and the equation for the lower velocity due to the buoyancy force. This system, as shown in the paper, can be represented in Hamiltonian form by means of the Poisson brackets. One of the results is the three closed ordinary differential equations (10) for mean characteristics. This system generalizes the virial theorem. The other interesting result concerns construction of the collapsing isotropic solution with self-similar behavior and anisotropic collapsing solution with self-similar asymptotics. In the first case the solution describes the formation of the point singularity in a finite time, while the latter situation describes the formation of singularity on the whole interval.

The main goal of this paper was to study structural elements of collapses in the shallow-water model with horizontally nonuniform density. The diagram of stability based on the rigorous integral criterion for isotropic collapse allows us to make some qualitative conclusions about system behavior in the space of constants of motion. In particular, depending on the ratio between two integrals of motion V_0 and m, an amplification of rotation, i.e., an increase in the angular velocity Ω leads both to stabilization, if $|V_0| < |m|$, and to destabilization of the flow, if $|V_0| \geqslant |m|$.

In our opinion, the collapse phenomenon arises at the final stage when the development of instability has led to disintegration of the strongly perturbed flows. Once the fluid forms localized (droplike) fragments, the collapse eventually occurs and leads to the formation of finite-time singularities.

Analysis of the instability shows that two collapse scenarios are possible depending on whether the contact area between the drop and the bottom is contractible into a segment or into a point. In the course of anisotropic collapsing, the contact area contracts into a spinning segment and the drop height h obeys the law $h \sim (t_0 - t)^{-2/3}$. In contrast, the isotropic scenario implies that the contact area contracts into a point. Because of this, height h follows relatively quicker laws $h \sim (t_0 - t)^{-1}$ and $h \sim (t_0 - t)^{-2}$ in warm and neutral regimes, respectively. In the absence of collapses, a droplike fragment undergoes nonlinear oscillations with the period equal to π/Ω. This period is the largest time scale of the rotating shallow-water system.

ACKNOWLEDGMENTS

This work was supported by the Russian Foundation for Basic Research (Project No. 12-05-00168), by the Presidium of the Russian Academy of Sciences (Program Fundamental Problems of Nonlinear Dynamics), and by the President of the Russian Federation (Program NSh-4166.2006.5). The authors are indebted to E. P. Tito for discussions and collaborations.

APPENDIX: FORMULATION OF MODEL

Consider two layers of inviscid incompressible fluids which move under the action of gravity g in the Cartesian frame x, y, z rotating around the vertical axis z with constant angular velocity $\mathbf{\Omega} = (0,0,\Omega)$. Suppose the layers are separated by surface $z = h(x,y,t)$ and are contained between two rigid parallel planes $z = 0$ and $z = l$ as shown in Fig. 9. Our purpose is to derive a description for this flow in the shallow-water approximation taking into account that density jump between the layers is small and horizontally nonuniform. Corresponding motion equations can be obtained from results [6] if the free boundary condition for the uppermost layer in Ripa's model is replaced by the rigid-lid approximation.

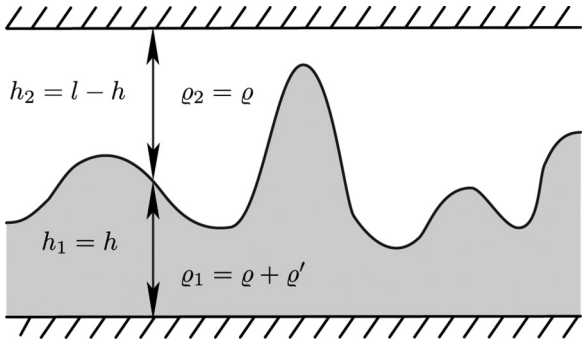

FIG. 9. The two-layer model of fluids between two rigid parallel horizontal planes in $z = 0$ and $z = l$.

This modification does not change Ripa's equations which, as before, take the form

$$(\partial_t + \mathbf{u}_i \cdot \nabla)\,\mathbf{u}_i - 2\boldsymbol{\Omega} \times u_i + \nabla \tilde{p}_i = \tilde{h}_i \nabla \theta_i, \tag{A1}$$

$$\partial_t h_i + \nabla \cdot (h_i \mathbf{u}_i) = 0, \quad (\partial_t + \mathbf{u} \cdot \nabla)\,\theta_i = 0 \tag{A2}$$

in each ith layer, where $h_i(x,y,t)$ is the thickness, $\mathbf{u}_i(x,y,t)$ is the velocity, $\theta_i(x,y,t) = \mathrm{g}\varrho_i/\varrho$ is the buoyancy, and the constant ϱ is a background density.

Note that variables $\mathbf{u}_i(x,y,t)$ and $\theta_i(x,y,t)$ must be interpreted as vertically layer-averaged quantities. Two other variables $\tilde{h}_i(x,y,t)$ and $\tilde{p}_i(x,y,t)$ are treated as the height of the center of mass of the layer and the effective pressure in the absence of inhomogeneities, respectively. In the rigid-lid approximation, Ripa's definition of $\tilde{h}_i$ remains unchanged:

$$\tilde{h}_i = \sum_{k=1}^{i} h_k - \frac{1}{2} h_i, \tag{A3}$$

but the definition for $\tilde{p}_i$ must be modified as

$$\tilde{p}_i = \theta_i \sum_{k=1}^{i} h_k + \sum_{k=i+1}^{n} \theta_k h_k + p', \tag{A4}$$

where n is the number of layers, $p'(x,y,t) \neq \text{const}$ is the rigid-lid pressure, and layer thicknesses satisfy the condition

$$\sum_{k=1}^{n} h_k = l, \tag{A5}$$

where the total depth l is a constant.

In the case of two layers, assuming $\varrho_2 = \varrho = \text{const}$ and $\varrho_1 = \varrho + \varrho'(x,y,t)$, we obtain in accordance with (A3)–(A5) that

$$\tilde{h}_1 = \frac{1}{2} h_1, \quad \tilde{h}_2 = h_1 + \frac{1}{2} h_2 = l - \frac{1}{2} h_2, \tag{A6}$$

$$\tilde{p}_1 = \theta_1 h_1 + \theta_2 h_2 + p', \quad \tilde{p}_2 = l\theta_2 + p', \tag{A7}$$

$$\theta_1 = \mathrm{g}\left(1 + \frac{\varrho'}{\varrho}\right), \quad \theta_2 = \mathrm{g}. \tag{A8}$$

After substitution of relations (A6)–(A8) into Eqs. (A1) and (A2), these equations take the form

$$(\partial_t + \mathbf{u}_1 \cdot \nabla)\,\mathbf{u}_1 - 2\Omega \times \mathbf{u}_1 + \nabla p' = -\frac{1}{2h_1} \nabla\left(h_1^2 \tau\right), \tag{A9}$$

$$(\partial_t + \mathbf{u}_2 \cdot \nabla)\,\mathbf{u}_2 - 2\Omega \times \mathbf{u}_2 + \nabla p' = 0, \tag{A10}$$

$$\partial_t h_1 + \nabla \cdot (h_1 \mathbf{u}_1) = 0, \tag{A11}$$

$$\partial_t h_2 + \nabla \cdot (h_2 \mathbf{u}_2) = 0, \tag{A12}$$

$$\partial_t \tau + \mathbf{u}_1 \cdot \nabla \tau = 0, \tag{A13}$$

where subscripts 1,2 show layer numbers. Note that the reduced gravity $\tau = \theta_1 - \theta_2 = \mathrm{g}\varrho'/\varrho$ may take any sign depending on the difference between positively defined quantities θ_1 and θ_2.

Because of condition $h_1 + h_2 = l$, from Eqs. (A12) one can find that

$$\nabla \cdot [h_1 \mathbf{u}_1 + (l - h_1)\mathbf{u}_2] = 0. \tag{A14}$$

Using (A14) and combining (A9) and (A10), it is easy to find the Poisson equation for the pressure distribution

$$\Delta\left(lp' + \tfrac{1}{2} h_1^2 \tau\right) = \partial_i \partial_j [h_1 u_{1i} u_{1j} + (l - h_1) u_{2i} u_{2j}]. \tag{A15}$$

Here Δ is the Laplacian. Let U be the scale of the velocity $\mathbf{u}_1$, L be the horizontal length scale, and $h_1 \ll l$, so $\varepsilon = h_1/l$ is a small parameter. Then, if $O(h_1 \tau/U^2) = 1$, from (A14) and (A15) we have estimations

$$\mathbf{u}_2 = O(\varepsilon U), \quad p' = O(\varepsilon U^2).$$

This result allows us to eliminate pressure gradient $\nabla p'$ from Eq. (A9). Thus, using the thin-layer approximation and omitting the layer subscript, we obtain, in the leading order, the closed system of equations (1)–(3).

[1] S. Chandrasekhar, *Hydrodynamic and Hydromagnetic Instability* (Clarendon, Oxford, 1961).
[2] N. J. Mueschke, M. J. Andrews, and O. Schilling, J. Fluid Mach. **567**, 27 (2006).
[3] N. J. Mueschke and O. Schilling, Phys. Fluids **21**, 014106 (2009).
[4] N. J. Mueschke and O. Schilling, Phys. Fluids **21**, 014107 (2009).
[5] J. E. Simpson, Annu. Rev. Fluid Mech. **14**, 213 (1982).
[6] P. Ripa, Geophys. Astrophys. Fluid Dyn. **70**, 85 (1993).
[7] T. Foglizzo, F. Masset, J. Guilet, and G. Durand, Phys. Rev. Lett. **108**, 051103 (2012).
[8] P. A. Gilman, Astrophys. J. **544**, L79 (2000).
[9] D. A. Schecter, J. F. Boyd, and P. A. Gilman, Astrophys. J. **551**, L185 (2001).
[10] E. A. Kuznetsov, Chaos **6**, 381 (1996).
[11] E. A. Kuznetsov and V. E. Zakharov, Lect. Notes Phys. **542**, 3 (2000).
[12] E. A. Kuznetsov, Physica D **184**, 266 (2003).
[13] E. A. Kuznetsov, Radiophys. Quantum Electron. **46**, 307 (2003).

[14] E. A. Kuznetsov, Top. Appl. Phys. **114**, 175 (2009).
[15] V. E. Zakharov and E. A. Kuznetsov, Phys. Usp. **55**, 535 (2012).
[16] J. Eggers and M. A. Fontelos, Nonlinearity **22**, R1 (2009).
[17] V. P. Goncharov and V. I. Pavlov, *Hamiltonian Vortex and Wave Dynamics* (Geos, Moscow, 2008) (in Russian).
[18] V. P. Goncharov, JETP Lett. **89**, 393 (2009).
[19] V. P. Goncharov, JETP **113**, 714 (2011).
[20] V. P. Goncharov and V. I. Pavlov, JETP Lett. **84**, 384 (2006).
[21] V. Goncharov and V. Pavlov, Phys. Rev. E **76**, 066314 (2007).
[22] V. P. Goncharov and V. I. Pavlov, JETP, **111**, 124 (2010).
[23] V. P. Goncharov and V. I. Pavlov, JETP Lett. **96**, 474 (2012).
[24] E. A. Kuznetsov, JETP Lett. **80**, 83 (2004).
[25] E. A. Kuznetsov, V. Naulin, A. H. Nielsen, and J. J. Rasmussen, Phys. Fluids **19**, 105110 (2007).
[26] The physics of local collapse in stars obviously involves complex ingredients such as nuclear physics, neutrino interactions, multidimensional hydrodynamics, and in some cases, general relativity. However, current understanding of the phenomenon is based on simplified formulations which help make the problem, at minimum, numerically tractable, if not physically intuitive. Drawing a parallel between stellar phenomena and geophysical consideration or SWL physics is perhaps unexpected, but has its roots in the universality of the laws of fluid mechanics.
[27] G. I. Barenblatt, *Scaling, Self-Similarity, and Intermediate Asymptotics* (Cambridge University Press, Cambridge, 1996).
[28] E. Fermi, *Collected Papers of Enrico Fermi* (University of Chicago Press, Chicago, 1965), Vol. II, Chap. 243, p. 813; Chap. 244, p. 816; Chap. 245, p. 821.
[29] D. L. T. Anderson, Tellus, Ser. A **36**, 278 (1984).
[30] P. S. Schopf and M. A. Cane, J. Phys. Oceanogr. **13**, 917 (1983).
[31] B. A. Trubnikov, S. K. Zhdanov, and S. M. Zverev, *Hydrodynamics of Unstable Media: General Theory and Applied Problems* (CRC Press, Boca Raton, 1996).
[32] P. J. Dellar, Phys. Fluids **15**, 292 (2003).
[33] S. N. Vlasov, V. A. Petritshchev, and V. I. Talanov, Radiophys. Quantum Electron. **14**, 1062 (1971).
[34] V. E. Zakharov and E. A. Kuznetsov, Zh. Eksp. Teor. Fiz. **91**, 1310 (1986) [Sov. Phys. JETP **64**, 773 (1986)].